



HAL
open science

Conjunction Observations of Energetic Oxygen Ions O^+ Accumulated in the Sequential Flux Ropes in the High-Altitude Cusp

Suping Duan, Lei Dai, Chi Wang, Chunlin Cai, Zhaohai He, Yongcun Zhang, H. Rème, I. Dandouras

► To cite this version:

Suping Duan, Lei Dai, Chi Wang, Chunlin Cai, Zhaohai He, et al.. Conjunction Observations of Energetic Oxygen Ions O^+ Accumulated in the Sequential Flux Ropes in the High-Altitude Cusp. *Journal of Geophysical Research Space Physics*, 2019, 124 (10), pp.7912-7922. 10.1029/2019JA026989 . hal-02408921

HAL Id: hal-02408921

<https://hal.science/hal-02408921>

Submitted on 13 Dec 2019

HAL is a multi-disciplinary open access archive for the deposit and dissemination of scientific research documents, whether they are published or not. The documents may come from teaching and research institutions in France or abroad, or from public or private research centers.

L'archive ouverte pluridisciplinaire **HAL**, est destinée au dépôt et à la diffusion de documents scientifiques de niveau recherche, publiés ou non, émanant des établissements d'enseignement et de recherche français ou étrangers, des laboratoires publics ou privés.

31 3) Conjunction observations present sequential FTEs transfer from the dayside LLBL to the cusp.

32

33 **1. Introduction**

34 The cusp is one of important source regions of single charge oxygen ions, O^+ , in the
35 magnetosphere. The outflow of oxygen ions can be observed in the whole cusp region [e.g., Yau et
36 al., 1985; Yau and Andre, 1997; Yau et al., 2007]. The energy of the outflow oxygen ions is around
37 300 eV at the middle altitude cusp [e.g., Yau et al., 2007]. But oxygen ions with energy above 1
38 keV have been observed in the high altitude cusp regions [e.g., Slapak, et al., 2011; Kristler, et al.,
39 2010]. There are many debates on the source of energetic oxygen ions in the high altitude cusp
40 region [e.g., Chen and Fritz, 2001; Fritz et al., 2003; Lindstedt et al., 2011; Trattner et al., 2011].
41 Lindstedt et al. [2010] proposed that the oxygen ions can be locally accelerated by the
42 perpendicular electric field in the high altitude cusp. Chen and Fritz [2001] reported that energetic
43 oxygen ions were from the ionosphere and energized at the high altitude cusp. On the other hand,
44 Trattner et al. [2011] pointed out that the energetic oxygen ions were originated from the forth
45 shock ahead magnetosheath.

46

47 The Flux Transfer Events (FTEs) originated from the low latitude dayside magnetopause can
48 move along the magnetopause to the high latitude cusp region [e.g., Akhavan-Tafti et al., 2018;
49 Cowley 1982; Lee and Fu, 1985; Roux et al., 2015]. Flux ropes or open flux tubes are usually
50 adopted as the description of FTEs [e.g., Duan et al., 2015; Eastwood et al., 2016; Lee and Fu,
51 1985; Roux et al., 2015, Sun et al., 2019; Xiao et al., 2004; Zhang et al., 2010]. Lee and Fu [1985]
52 reported that multiple X-line reconnection gave rise to multiple flux ropes at the dayside
53 magnetopause. Omidi and Sibeck [2007] proposed that multiple FTEs with a various sizes are
54 formed at LLBL and traveled along the magnetopause surface into high latitude polar region
55 during southward IMF. The periodicity of sequential FTEs is in the range from 1.5 min to 18.5
56 min with average value of 8 min and common value of 3 min [e.g., Trattner et al., 2012; Rijnbeek
57 et al., 1984; Lockwood and Wild, 1994]. Cowley [1982] reported that the travel time of FTEs from
58 the subsolar magnetic reconnection region to the vicinity of the cusp was around 5 min. The low
59 latitude flux ropes propagate towards southward and northward high latitude region with different
60 bipolar signatures [e.g., Berchem and Russell, 1984; Le et al., 2008]. Le et al. [2008] pointed out

61 that the southward moving flux tube produced a bipolar signature with inward/outward (-/+)
62 polarity.

63

64 The scale size of flux ropes at the dayside magnetopause is in the range from a few hundred
65 kilometers to about an Earth radius [e.g., Akhavan-Tafti et al., 2018; Lee and Fu, 1985; Eastwood
66 et al., 2016; Sun et al., 2019]. Akhavan-Tafti et al. [2018] reported that the mean diameter of FTEs
67 was ~1700km at the Earth's subsolar magnetopause. Eastwood et al. [2016] reported that ion-scale
68 flux ropes with scale size ~1100 km were observed by MMS at the dayside magnetopause. Ten
69 keV energetic oxygen ions near the dayside magnetopause have gyroradius around ~1000 km.
70 These energetic oxygen ions may be captured into the flux ropes and transported from low latitude
71 to high latitude region. Phan et al. [2004] reported that energetic O⁺ with energy larger than 3keV
72 in the reconnection jets are observed by Cluster at the duskside mid-latitude magnetopause under
73 steady southward IMF condition.

74

75 In this paper, the conjunction observations of TC-1 and Cluster present a clear chain for sequential
76 FTEs transport from the LLBL to the high altitude cusp. We focus on the sequential FTEs
77 accumulated with energetic oxygen ions in the high altitude cusp observed by Cluster. They both
78 observed sequential FTEs with interval time period of ~ 3 min. In the second section the
79 observations of sequential FTEs near the dayside magnetopause by TC-1 and FTEs accumulated
80 with energetic oxygen ions in the high altitude cusp by Cluster are presented, respectively.
81 Discussions and summary are shown in the last section.

82

83 **2. Conjunction observations of FTEs**

84 **2.1 Sequential Flux ropes observed by TC-1 at the LLBL**

85 Figure 1 shows plasma and magnetic field data from TC-1 located near the dayside magnetopause.
86 From top to bottom, the panels show that (a) ions number density, (b) ions temperature, (c) plasma
87 beta value β , (β is the ratio of plasma thermal pressure to the magnetic pressure, $\beta=2\mu_0nT/B^2$), (d)
88 to (f) the x, y, and z component of ions velocity, (g) to (i) the z, x, and y component (grey line) and
89 the total magnitude (black line) of magnetic field. The position of TC-1 located near dayside low
90 latitude magnetopause is presented at the bottom in Figure 1. The two vertical red lines mark the

91 time intervals of the continuous negative B_z component from 10:53:00 UT to 11:14:00 UT. The
92 minimum value of B_z component is about - 40 nT. During this interval the ions number density is
93 high (larger than 10 cm^{-3}) as shown in Figure 1a. The maximum value of ion number density is
94 about 25 cm^{-3} . Ion temperature is low (less than 1 keV) as shown in Figure 1b. Ions velocity in the
95 X direction is negative and slow, $V_x \sim -100 \text{ km/s}$. Those parameters indicate that TC-1 is located
96 at the dayside magnetosheath-side of the low latitude boundary layer. Figure 1f presents that the
97 B_x component has bipolar signatures. This may be associated with the magnetic reconnection at
98 the dayside magnetopause. So we display the magnetic field and ions velocity in the local
99 boundary normal coordinate system (LMN) in Figure 2.

100

101 Figure 2 shows three components of the magnetic field and proton velocity in LMN coordinate
102 system. From top to bottom, the panels display the B_N , B_M , B_L component, and the total
103 magnitude B_t of the magnetic field, the v_N, v_M, v_L component and the total magnitude v_t of the ions
104 velocity, respectively. The normal vector $\mathbf{N} = (0.93, 0.26, -0.25)$ (GSM) is determined as the
105 minimal variation direction of the magnetic field in the interval from 10:56:50 UT to 10:59:56 UT.
106 The vectors \mathbf{M} and \mathbf{L} are defined as $\mathbf{M} = \mathbf{N} \times \mathbf{Z}_{\text{GSM}}$ and $\mathbf{L} = \mathbf{M} \times \mathbf{N}$. In Figure 2 three green shade
107 regions demonstrate that the B_N firstly decreases then increases, the B_M sharply increases and the
108 significant increase in the magnetic total value, B_t . These three regions mark three flux ropes
109 observed by TC-1 near the dayside low-latitude magnetopause. They are signed as FR_{A1} , FR_{B1} and
110 FR_{C1} shown at the topside of Figure 6, respectively. The first flux rope marked by FR_{A1} has large
111 negative B_N then decrease suddenly at 10:52:20 UT. The second and third flux ropes marked by
112 FR_{B1} and FR_{C1} have distinct B_N bipolar signature from negative to positive and larger total value
113 of magnetic field at 10:56:20 UT and 10:58:50 UT respectively. The location of TC-1, \sim
114 $(10.51, -0.28, -1.57) R_E$, at the bottom of Figure 2 shows that the spacecraft located in the
115 southward hemisphere side of subsolar point. The negative to positive bipolar signatures imply
116 that flux ropes are from the subsolar point magnetic reconnection and propagate toward the
117 southward hemisphere [Le et al., 2008]. These three flux ropes are all accompanied with down-tail
118 ions bulk flow, as shown in Figure 2e and 2g.

119

120 **2.2 Energetic oxygen ions within Sequential Flux ropes in the high-altitude cusp**

121 Figure 3 presents the plasma and magnetic field observed by Cluster C4 at southern hemisphere
122 high latitude region around (3.7,-4.4,-9.8) Re. From top to bottom, the panels show the number
123 density of (a) proton, (b) helium ions He^{++} , and (c) oxygen ions O^+ , (d) proton temperature, (e)
124 plasma beta value, β , (f) the x component of proton velocity, (g) to (i) the x and z component of
125 the magnetic field, the magnetic field total magnitude (black line) and the B_y component (blue
126 line), respectively. During the intervals of 10:57 UT to 11:09 UT, Figure 3b presents that the He^{++}
127 number density is larger than 0.5 cm^{-3} . At the same time period, Figure 3f displays the proton v_x
128 component value decrease to around $\sim 100 \text{ km/s}$ and in the tailward direction. Figure 3i shows the
129 total magnetic field magnitude decreases and with significant fluctuations. Those parameters
130 demonstrate that Cluster C4 is crossing the high altitude cusp. At 10:57:30 UT, the B_x and B_z
131 components change from positive value to negative value which as marked by the first pink
132 vertical dashed line. After this time Cluster C4 enters into the southern high altitude cusp region.
133 Figure 3c presents three sharp increases in the number density of O^+ ions in the high altitude cusp,
134 as marked by three vertical red lines in Figure 3. The maximum value of O^+ ions number density
135 is about 0.27 cm^{-3} in the cusp. Corresponding these oxygen ions number density increase, the
136 magnetic field total value also increases and the B_z component has bipolar signature as shown in
137 the last two panels, Figure 3i and 3h, respectively.

138

139 Figure 4 presents the oxygen ions energy flux spectrum and pitch angle distribution in the
140 intervals of 10:30 UT to 11:30 UT. The first panel shows the oxygen ions energy flux from 40 eV
141 to 40 keV. The next three panels show oxygen ions pitch angle distributions in three energy
142 channel 40 eV to 1 keV, 1 keV to 10 keV, 10 keV to 40 keV, respectively. The interval between the
143 two pink vertical dashed lines is the time of Cluster crossing the high altitude cusp. Figure 4a
144 clearly demonstrates that energetic oxygen ions with energy larger than 10 keV are found in the
145 high altitude cusp region. They are especially marked by the three dotted vertical lines in Figure 4.
146 The pitch angle distribution of high energy oxygen ions, $>10 \text{ keV}$, presented in Figure 4d, shows
147 that these O^+ ions are dominated in the pitch angle less than 90 degree. It means that those O^+ ions
148 almost outflow from the low altitude cusp in the southern hemisphere. On the other hand, oxygen
149 ions with energy less than 10 keV are distributed in a wide pitch angle range from 0 to 180 degree,
150 as shows in Figure 4b and 4c. According to the energetic O^+ ions with sharp increase in the

151 energy flux and number density, we present the magnetic field and proton velocity in the LMN
152 coordinate system in the cusp, as shown in Figure 5.

153

154 Figure 5 presents three flux ropes observed by Cluster C4 in the high altitude cusp region, which
155 are marked by three green shade regions, FR_A, FR_B and FR_C (shown at the topside of this figure) ,
156 respectively. From top to bottom, the panels show oxygen ions density, helium ions density, three
157 components of the magnetic field and proton velocity in a LMN coordinate system, B_N, B_M and
158 B_L, v_N, v_M and v_L, respectively. The normal vector $\mathbf{N} = (-0.43, 0.02, 0.90)$ (GSM) is determined as
159 the minimal variation direction of the magnetic field in the intervals from 11:00:45 UT to 11:01:45
160 UT. Figure 5a shows that these three flux ropes are accumulated within the high density of oxygen
161 ions, $n_{O^+} \sim 0.25 \text{ cm}^{-3}$, in the high altitude cusp. The B_N component has bipolar signals at around
162 10:58:20UT, 11:02:20UT and 11:04:50UT, as shown in Figure 5c. The total magnetic magnitude
163 increases significantly at these three times, as presented in Figure 5f. These flux ropes all have
164 negative v_L value as shown in the bottom panel. These features of the magnetic field show that
165 three flux ropes are observed in the high altitude cusp regions with a period of ~ 3 min.

166

167 The wide range of the pitch angle distribution of energetic oxygen ions in the high altitude
168 cusp shown in Figure 4b and 4c means that these oxygen ions are from two different regions.
169 The 2D cut of oxygen ions velocity distributions can clearly reveal that the energetic O⁺ ions are
170 characterized with the counter-streaming flows. Figure 6 shows the velocity distributions of
171 oxygen ions with energy in the range of 40 eV to 40 keV at 10:59:24 UT, 11:02:28 UT and
172 11:05:53 UT, respectively. Within these three flux ropes oxygen ions have counter-streaming
173 features, which are both presented in Figure 6b and 6c. The right three panels of Figure 6
174 show that oxygen ions have large counter-direction velocity in the Z direction at 10:59:24
175 UT, 11:02:28 UT and 11:05:53 UT respectively. The total magnitude of O⁺ ions velocity is
176 around 600 km/s. These three times are in the time intervals of the magnetic flux ropes in the
177 high altitude cusp region which are shown in Figure 5 as three green shade regions,
178 respectively. They have one-to-one corresponding relationship. These counter-streaming
179 oxygen ions in three flux ropes demonstrate that they are from two different regions. They
180 consist of the ionosphere outflow and magnetopause magnetic reconnection precipitation.

181

182 **3. Summary and discussions**

183 The above conjunction observations of TC-1 at the LLBL and Cluster at the high altitude cusp
184 regions are adopted to investigate the sequential FTEs transporting from the subsolar dayside
185 magnetopause to the high altitude cusp. The results demonstrate that the energetic oxygen ions
186 have counter-streaming in the high altitude cusp regions. These oxygen ions have two different
187 source origins. One is from the ionosphere outflow. The other is the oxygen ions precipitation
188 originating from the magnetic reconnection region at the low latitude dayside magnetopause. As
189 displayed in Figure 5, there are three flux ropes observed by Cluster C4 at high-altitude cusps
190 about ~5-6 minutes delay from those by TC-1 at 10:58:20 UT, 11:01:20 UT and 11:04:50 UT,
191 respectively, which are presented by three green shaded regions marked by FR_A, FR_B and FR_C,
192 respectively. Thus, these conjunction observations of sequential FTEs suggest that the
193 high-latitude Flux ropes in the cusp are from the dayside low-latitude magnetopause reconnection.
194 On the other hand, the velocity distributions in these flux ropes as shown in Figure 6 present ions
195 precipitation in the high-altitude cusps with the large v_z value. Ions precipitation along the
196 magnetic field has been used to induce the magnetic reconnection process. The ions precipitation
197 also implies that these three cusp flux ropes are origin from the dayside low-latitude
198 magnetopause reconnections. Phan et al. [2004] reported that energetic oxygen ions with high
199 density $0.2-0.3 \text{ cm}^{-3}$ in the reconnection jets are observed by Cluster at the dayside magnetopause
200 under the steady southward IMF. Our results that the sequential FTEs accumulated with high
201 number density 0.25 cm^{-3} of energetic oxygen ions in the high altitude cusp maybe associated with
202 the similar reconnection at the LLBL reported by Phan et al. [2004].

203

204 The delay time ~ 5-6 min from the LLBL flux ropes (FR_{A1}, FR_{B1} and FR_{C1}) observed by TC-1 to
205 the high altitude cusp flux ropes (FR_A, FR_B and FR_C) observed by Cluster is consisted with the
206 propagating time of FTEs from LLBL to cusp in previous reports [e.g., Cowley, 1982]. According
207 to TC-1 observations, the background magnetic field magnitude 60 nT and the ions density 16 cm^{-3}
208 as presented in Figure 1i and 1a, the Alfvén speed can be calculated is ~ 327 km/s. Based on the
209 locations of TC-1 at the bottom of Figure 1, TC-1 observed FTEs at the LLBL with $X \sim 10.4 R_E$,
210 we can calculate the time interval of FTEs transporting from the LLBL to the high altitude cusp

211 being ~ 5.3 min. This calculating time interval of FTEs transporting from the LLBL to the high
212 altitude cusp is consistent with that of conjunction observations between TC-1 at the LLBL and
213 Cluster in the cusp time intervals, from 10:52:20 UT to 10:58:40 UT, 10:56:20 UT to 11:01:20 UT
214 and 10:58:50 UT to 11:04:50 UT.

215

216 Energetic oxygen ions with tens keV energy have large Larmor radius, ~ several thousand km, in
217 the high altitude cusp. This spatial scale is closed to FTEs radius size in a few thousands km.
218 Those energetic oxygen ions can be trapped in these flux ropes and move along the magnetopause
219 to the high altitude cusp with the same velocity of FTEs. Eastwood et al. [2016] reported that
220 ion-scale flux ropes with ~1100 km generated by the magnetic reconnection are observed by MMS
221 at dayside low latitude magnetopause. Using 2.5-D global hybrid simulations, Omid and Sibeck
222 [2007] proposed that multiple FTEs with a various sizes are formed at LLBL and traveled along
223 the magnetopause surface into high latitude polar region during southward IMF. The energetic
224 oxygen ions in our event maybe origin from ring current during the recovery phase of the median
225 storm on 9 March, 2004 (Dst ~-80 nT). They escape into the low latitude magnetopause by
226 guiding center magnetic field. These energetic oxygen ions located in flux ropes as the
227 reconnection jets. The energetic oxygen ions with high number density observed in the
228 reconnection jet are also reported by Phan et al. [2004]. Tens keV energetic oxygen ions with large
229 gyroradius of ~ 1000km, which is close the radius of flux ropes, are trapped in FTEs propagating
230 to high latitude cusp and then to high latitude magnetotail region. Duan et al. [2015] reported that
231 flux ropes accumulated with energetic oxygen ions observed by Cluster at high latitude nightside
232 magnetotheath were from the high altitude cusp.

233

234 As addressed above, the conjunction observations of the sequential flux ropes at the low latitude
235 boundary layer by TC-1 and at the high altitude cusp by Cluster are investigated in our paper. The
236 main conclusions of our observations can be drawn as follows. The delay time of these sequential
237 flux ropes from the low latitude magnetopause to the high altitude cusp is around 5-6 min. These
238 sequential flux ropes are accumulated with energetic oxygen ions observed by Cluster in the high
239 altitude cusp. The number density of energetic O⁺ ions, detected by CIS/CODF instrument on
240 Cluster, is very high in these sequential flux ropes, ~ 0.25 cm⁻³. These O⁺ ions with different

241 energy have different pitch angle distribution in the high altitude cusp. The oxygen ions with
242 energy larger than 10 keV are dominantly distributed in the quasi-parallel direction along the
243 background magnetic field in the southern high altitude cusp. While O⁺ ions with lower energy
244 less than 10 keV have a wide range of pitch angle distribution from 0 degree to 180 degree. This
245 reveals that oxygen ions with energy less than 10 keV in the high altitude cusp are from two
246 different regions, the dayside low latitude magnetopause and low altitude cusp region. Our
247 investigations present evidence that the sequential flux ropes at dayside low latitude magnetopause
248 can carry oxygen ions into the high altitude cusp region.

249

250 **Acknowledgments**

251 We acknowledge the use of data from the ESA Cluster Science Archive ([http://www.cosmos.esa.](http://www.cosmos.esa.int/web/csa)
252 [int/web/csa](http://www.cosmos.esa.int/web/csa)). We thank the FGM, CIS, EFW instrument teams. This work is supported by the
253 National Natural Science Foundation of China grants 41874196, 41731070, 41574161 and
254 41574159; the Strategic Pioneer Program on Space Science, Chinese Academy of Sciences, grants
255 XDA15052500, XDA15350201 and XDA15011401; the NSSC Research Fund for Key
256 Development Directions and in part by the Specialized Research Fund for State Key Laboratories.

257

258 **References**

261 Akhavan-Tafti, M., Slavin, J. A., Le, G., Eastwood, J. P., Strangeway, R. J., Russell, C. T., et al.
262 (2018). MMS examination of FTEs at the Earth's subsolar magnetopause. *Journal of Geophysical*
263 *Research: Space Physics*, 123, 1224–1241. <https://doi.org/10.1002/2017JA024681>
264 Berchem, J., and C. T. Russell (1984), Flux transfer events on the magnetopause: Spatial
265 distribution and controlling factors, *J. Geophys. Res.*, 89, 6689.
266 Chen, J., and Fritz, T.A., (2001), Energetic oxygen ions of ionospheric origin observed in the cusp.
267 *Geophysical Research Letters* 28, 1459–1462.
268 Cowley, S.W.H., The causes of convection in the Earth's magnetosphere: A review of
269 developments during IMS, *Rev. Geophys.*, 20, 531, 1982.
270 Duan, S., L. Dai, C. Wang, A. T. Y. Lui, Z. Liu, Z. He, Y. Zhang, I. Dandouras, and H. Reme
271 (2015), Cluster observations of unusually high concentration of energetic O⁺ carried by flux ropes
272 in the nightside high-latitude magnetosheath during a storm initial phase, *J. Geophys. Res. Space*

273 Physics, 120, doi:10.1002/2015JA021306.

274 Eastwood, J. P., et al. (2016), Ion-scale secondary flux ropes generated by magnetopause
275 reconnection as resolved by MMS, *Geophys. Res. Lett.*, 43,4716–4724,
276 doi:10.1002/2016GL068747.

277 Fritz, T. A., J. Chen, and G. L. Siscoe (2003), Energetic ions, large diamagnetic cavities, and
278 Chapman-Ferraro cusp, *J. Geophys. Res.*, 108(A1), 1028, doi:10.1029/2002JA009476.

279 Kistler, L. M., C. G. Mouikis, B. Klecker, and I. Dandouras (2010), Cusp as a source for oxygen
280 in the plasma sheet during geomagnetic storms, *J. Geophys. Res.*, 115, A03209,
281 doi:10.1029/2009JA014838.

282 Lee, L. C., and Z. F. Fu (1985), A theory of magnetic flux transfer at the Earth's magnetopause,
283 *Geophys. Res. Lett.*, 12, 105.

284 Le, G., et al. (2008), Flux transfer events simultaneously observed by Polar and Cluster: Flux rope
285 in the subsolar region and flux tube addition to the polar cusp, *J. Geophys. Res.*, 113, A01205,
286 doi:10.1029/2007JA012377.

287 Lindstedt, T., Y. V. Khotyaintsev, A. Vaivads, M. André, H. Nilsson, and M. Waara (2010),
288 Oxygen energization by localized perpendicular electric fields at the cusp boundary, *Geophys. Res.*
289 *Lett.*, 37, L09103, doi:10.1029/2010GL043117.

290 Lockwood, M., and M. F. Smith (1994), Low and middle altitude cusp particle signatures for
291 general magnetopause reconnection rate variations: 1. Theory, *J. Geophys. Res.*, 99, 8531 – 8553.

292 Lockwood, M., S. W. H. Cowley, and T. G. Onsager (1996), Ion acceleration at both the interior
293 and exterior Alfvén waves associated with the magnetopause reconnection site: Signatures in cusp
294 precipitation, *J. Geophys. Res.*, 101, 21,501 – 21,515.

295 Omid, N., and D. G. Sibeck (2007), Flux transfer events in the cusp, *Geophys. Res. Lett.*, 34,
296 L04106, doi:10.1029/2006GL028698.

297 Phan, T. D., Dunlop, M. W., Paschmann, G. et al. (2004), Cluster observations of continuous
298 reconnection at the magnetopause under steady interplanetary magnetic field conditions, *Ann.*
299 *Geophys.*, 22, 2355–2367.

300 Markidis, S., G. Lapenta, L. Bettarini, M. Goldman, D. Newman, and L. Andersson (2011),
301 Kinetic simulations of magnetic reconnection in presence of a background O⁺ population, *J.*
302 *Geophys. Res.*, 116, A00K16, doi:10.1029/2011JA016429.

303 Rijnbeek, R. P., S. W. H. Cowley, D. J. Southwood, and C. T. Russell (1984), A survey of dayside
304 flux transfer events, observed by the ISEE-1 and -2 magnetometers, *J. Geophys. Res.*, 89, 786.

305 Roux, A., P. Robert, D. Fontaine, O. Le Contel, P. Canu, and P. Louarn (2015), What is the nature
306 of magnetosheath FTEs?, *J. Geophys. Res. Space Physics*, 120, 4576–4595,
307 doi:10.1002/2015JA020983.

308 Slapak, R., Nilsson, H., Waara, M., André, M., Stenberg, G., and Barghouthi, I. A.: O+ heating
309 associated with strong wave activity in the high altitude cusp and mantle, *Ann. Geophys.*, 29,
310 931–944, doi:10.5194/angeo-29-931-2011, 2011.

311 Sun, T.R., Tang B.B., Wang C., Guo X.C. and Y. Wang (2019), Large-scale characteristics of flux
312 transfer events on the dayside magnetopause, *J. Geophys. Res. Space Physics*, 124,
313 <https://doi.org/10.1029/2018JA026395>

314 Trattner, K. J., S. M. Petrinec, S. A. Fuselier, K. Nykyri, and E. Kronberg (2011), Cluster
315 observations of bow shockenergetic ion transport through the magnetosheath into the cusp,*J.*
316 *Geophys. Res.*, 116, A09207, doi:10.1029/2011JA016617.

317 Trattner, K. J., S. M. Petrinec, S. A. Fuselier, N. Omid, and D. G. Sibeck (2012), Evidence of
318 multiple reconnection lines at the magnetopause from cusp observations, *J. Geophys. Res.*, 117,
319 A01213, doi:10.1029/2011JA017080.

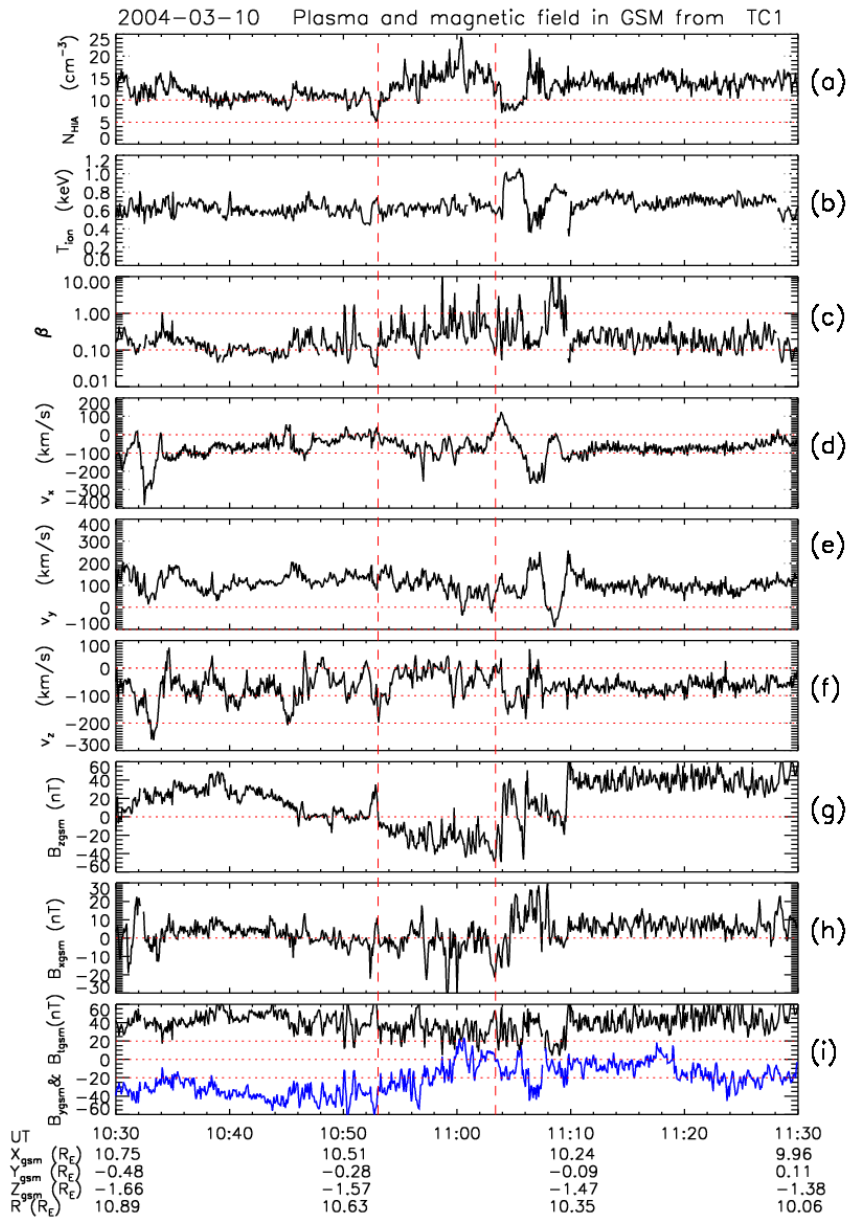
320 Yau, A. W., Shelley, E. G., Peterson, W. K., & Lenchyshyn, L. (1985). Energetic auroral and
321 polar ion outflow at DE 1 altitudes: Magnitude, composition, magnetic activity dependence, and
322 long-term variations. *Journal of Geophysical Research*, 90(A9), 8417–8432. [https://doi.](https://doi.org/10.1029/JA090iA09p08417)
323 [org/10.1029/JA090iA09p08417](https://doi.org/10.1029/JA090iA09p08417)

324 Yau, A. W., and M. Andre (1997), Sources of ion outflow in the high latitude ionosphere, *Space*
325 *Sci. Rev.*, 80, 1 – 25. .

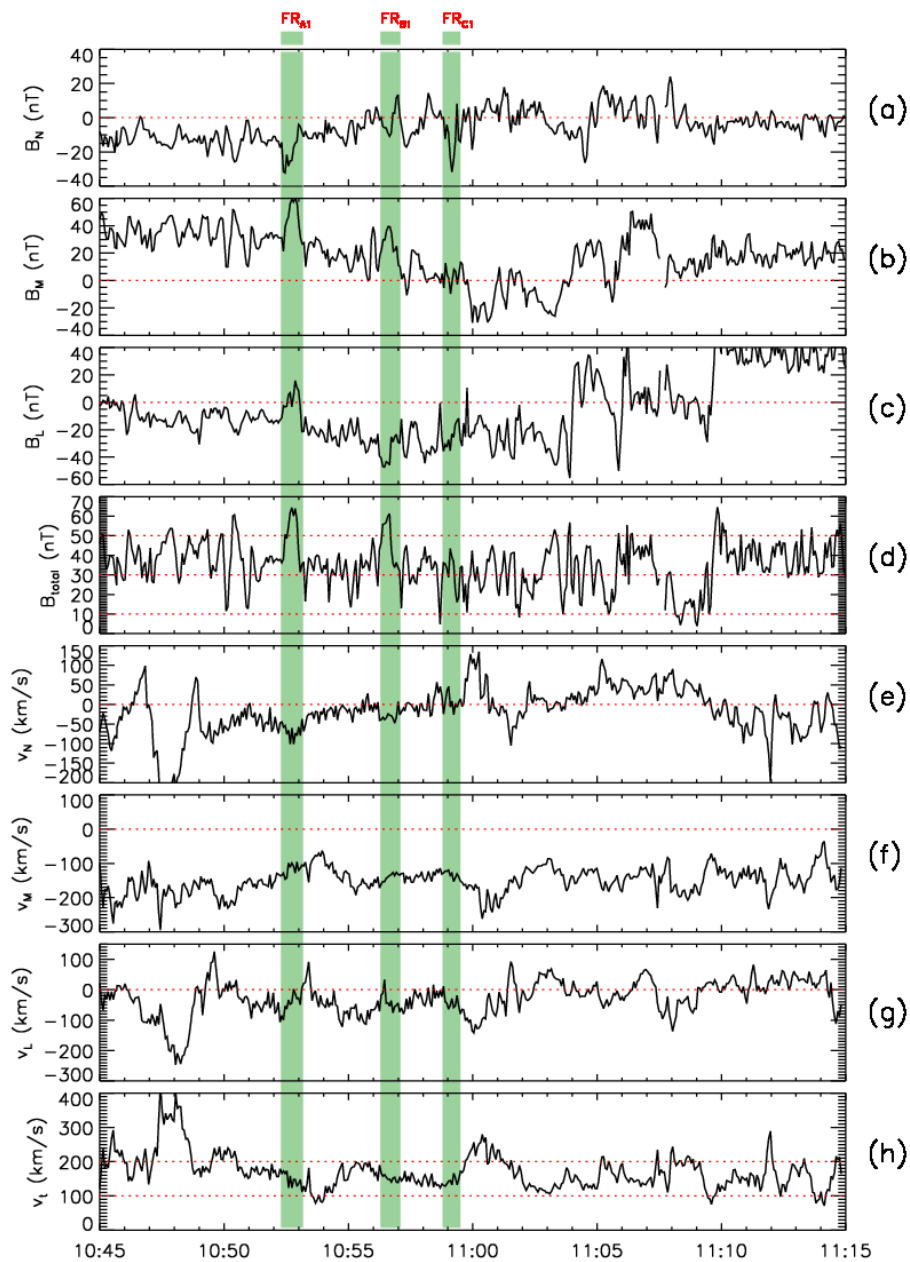
326 Yau, A. W., T. Abe, and W. K. Peterson (2007), The polar wind: Recent observations, *J. Atmos.*
327 *Sol. Terr. Phys.*, 69, 1936.

328 Xiao, C. J., Pu, Z. Y., Ma, Z. W., Fu, S. Y., Huang, Z. Y., & Zong, Q. G. (2004). Inferring of flux
329 rope orientation with the minimum variance analysis technique. *Journal of Geophysical Research*,
330 109, A11218. <https://doi.org/10.1029/2004JA010594>

331 Zhang, H., Kivelson, M. G., Khurana, K. K., McFadden, J., Walker, R. J., Angelopoulos, V., et al.
332 (2010). Evidence that crater flux transfer events are initial stages of typical flux transfer events.



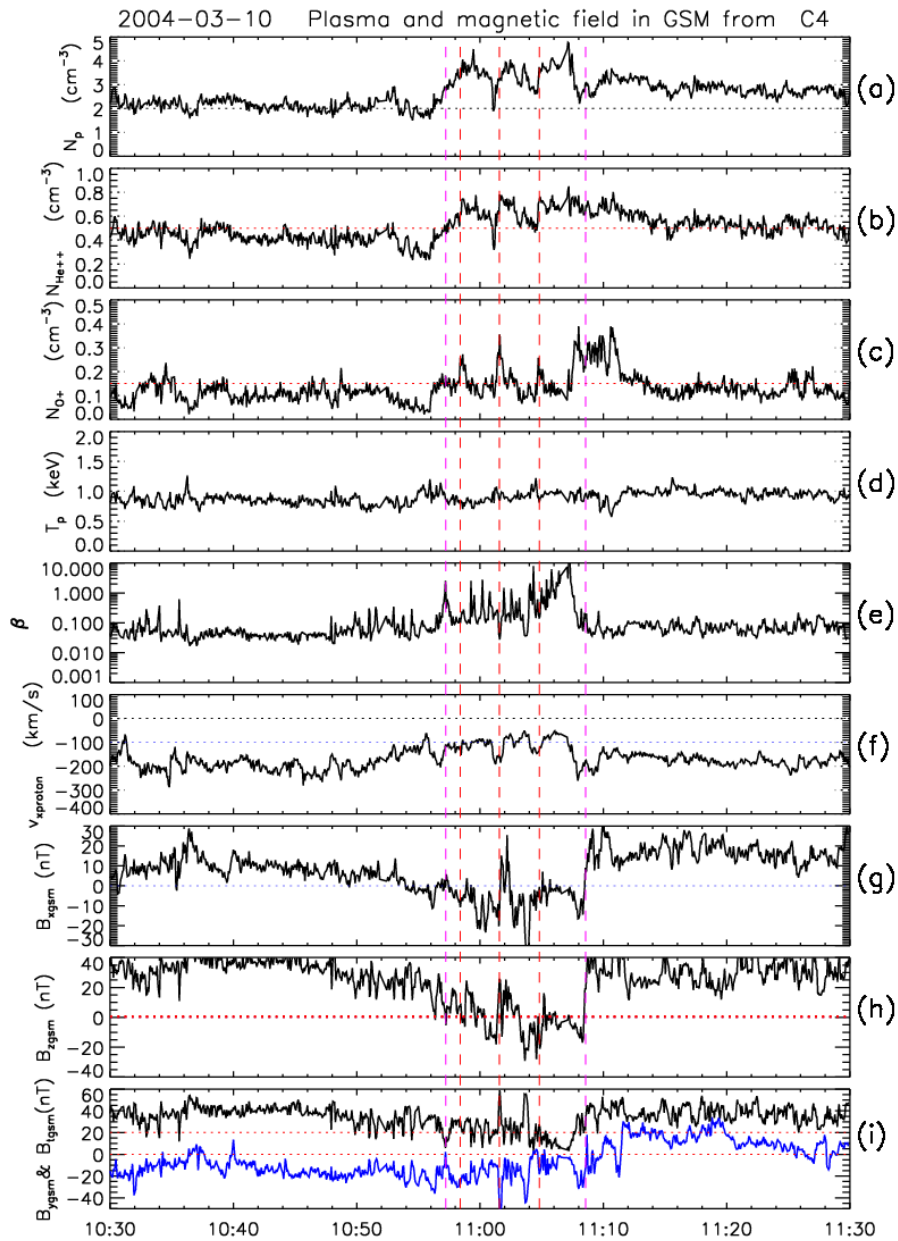
337 Figure 1 The plasma and magnetic field parameters are from TC-1 HIA and FGM during the
 338 period of 10:30 UT to 11:30 UT 10 March 2004. From top to bottom, panels are (a) ions number
 339 density, (b) ions temperature, (c) plasma beta value, β , (d) to (f) the v_x , v_y and v_z component of
 340 ions, respectively, (e) plasma beta value, β , (f) the x component of proton velocity, (g) the B_x
 341 component of magnetic field, (h) the B_z component, and (i) the B_y (blue line) and total magnitude
 342 of magnetic field.



344

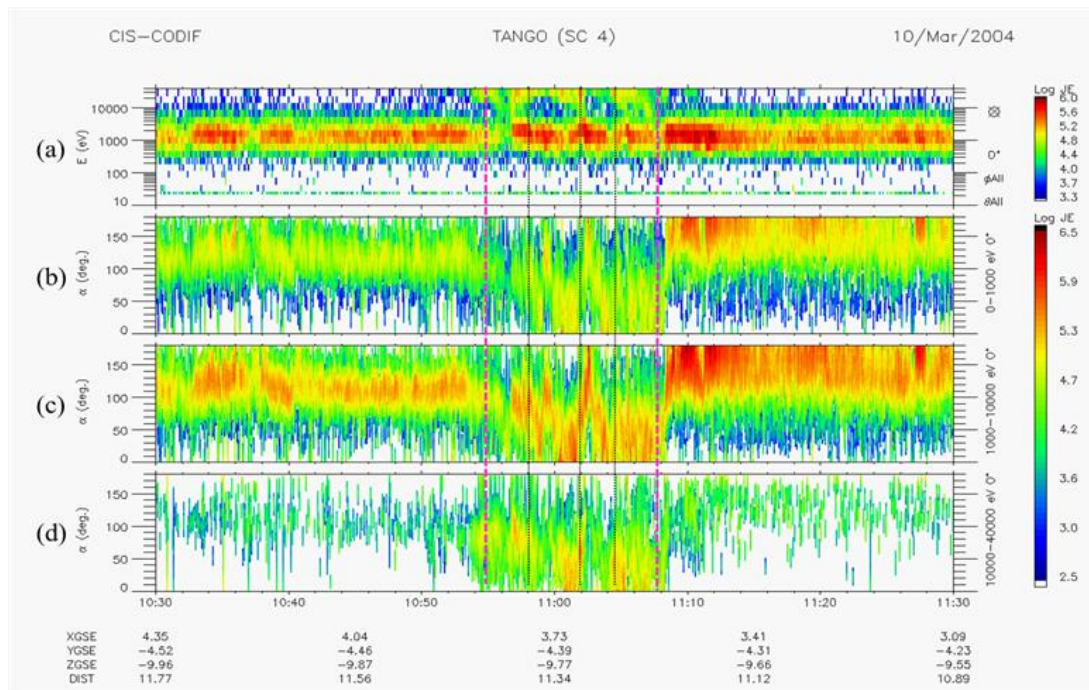
345 Figure 2 Sequential Flux ropes observed by TC-1 at the dayside low latitude boundary layer under
 346 the southward B_z component. From top to bottom, the panels are (a) the magnetic field B_N
 347 component, (b) the B_M component, (c) the B_L component, (d) the total magnitude of the magnetic
 348 field, B_t , (e) to (h) proton velocity v_N, v_M, v_L component and the total magnitude v_t , respectively.

349 Three green shade regions mark the intervals of sequential flux ropes observed by TC-1 at LBL
 350 as FR_{A1} , FR_{B1} , FR_{C1} at the top side of Figure 2, respectively.



351

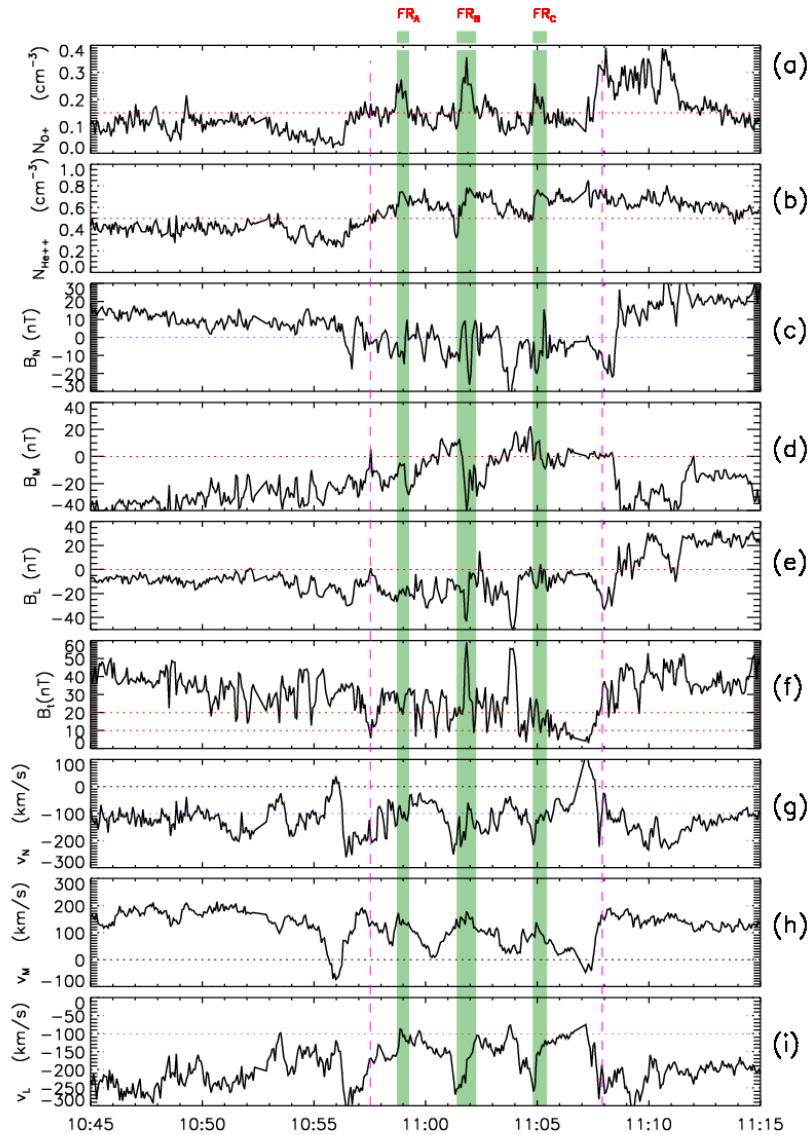
352 Figure 3 The plasma and magnetic field parameters are from Cluster C4 CIS/CODIF and FGM
 353 during the period of 10:30 UT to 11:30 UT 10 March 2004. From top to bottom, panels are (a)
 354 proton number density, (b) He^{++} number density, (c) O^+ number density, (d) proton temperature,
 355 (e) plasma beta value, β , (f) the x component of proton velocity, (g) the B_x component of magnetic
 356 field, (h) the B_z component, and (i) the B_y (blue line) and total magnitude of magnetic field. Three
 357 red dashed vertical lines mark the time of high number density of O^+ ions in the high altitude
 358 cusp.



360

361

362 Figure 4 The O^+ ion energy spectrogram flux and pitch angle distribution obtained from CODIF
 363 (energy range is from 40 eV to 40 keV) on 10 March 2004. (a) O^+ energy spectrogram of
 364 omnidirectional flux, (b) to (d) O^+ pitch angle distribution with energy in the range of 40 eV to 1
 365 keV, 1 keV to 10 keV, and 10 keV to 40 keV, respectively.

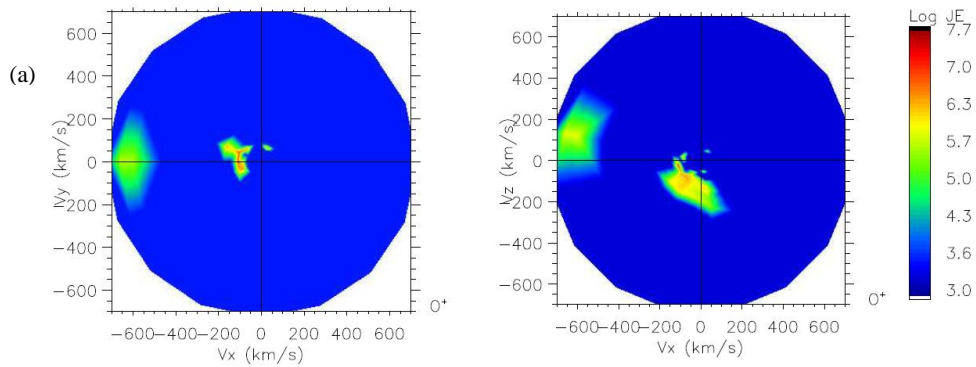


366

367 Figure 5 Sequential Flux ropes accumulated by energetic oxygen ions observed by Cluster
 368 C4 in southward high altitude cusp region, which are marked by FR_A , FR_B , FR_C at the top,
 369 respectively. From top to bottom, panels are (a) O^+ number density, (b) He^{++} number density,
 370 (c) the magnetic field B_N component, (d) the B_M component, (e) the B_L component, (f) the
 371 total magnitude B_t , (g) to (i) proton velocity v_N, v_M, v_L component, respectively. Three green
 372 shade regions mark the intervals of flux ropes and high number density of O^+ ions as FR_A ,
 373 FR_B , FR_C at the top of Figure 5, respectively.

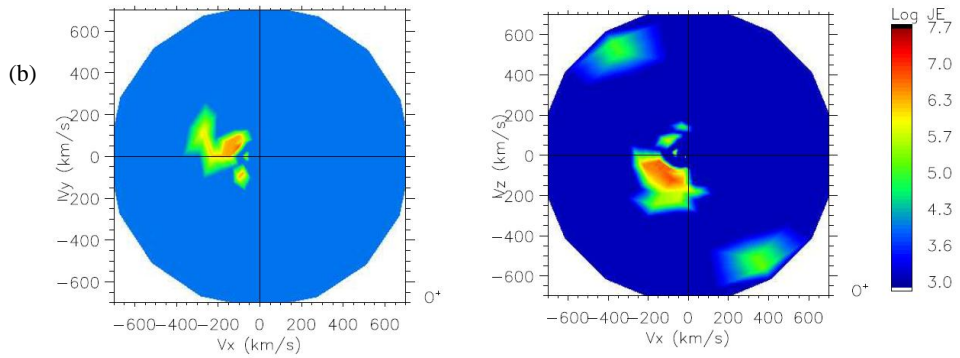
374

CIS-CODIF TANGO (SC 4) 10/Mar/2004 10:59:24.048



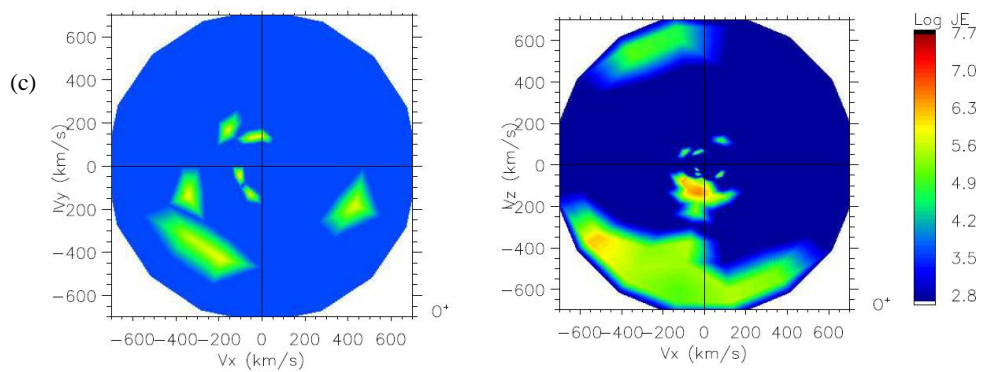
375

CIS-CODIF TANGO (SC 4) 10/Mar/2004 11:02:28.526



376

CIS-CODIF TANGO (SC 4) 10/Mar/2004 11:05:53.048



377

378 Figure 6 Two-dimensional cuts of the three-dimensional O^+ ion velocity distributions obtained by
 379 CODIF/C4 on 10 March 2004. Panels (a) to (c) show the O^+ ion velocity distributions in three flux
 380 ropes FR_A , FR_B , and FR_C at 10:59:24 UT, 11:02:28 UT, and 11:05:53 UT, respectively.

381